Electronic transmission through a set of metallic clusters randomly attached to an adsorbed nanowire: Localization-delocalization transition

V. Pouthier and C. Girardet
Laboratoire de Physique Moléculaire, UMR CNRS 6624, Faculté des Sciences–La Bouloie, Université de Franche-Comté, 25030 Besançon Cedex, France

(Received 16 May 2002; published 26 September 2002)

The electron transmission through a monatomic nanowire containing N attached quasiperiodically distributed nanoclusters is studied within the ballistic model. A decimation procedure is performed to renormalize the self-energy of the nanowire sites connected to the clusters and to transform the nanodevice into an effective disordered one-dimensional chain. The transmittance is determined using the transfer matrix formalism. It allows us to express each elementary reflection/transmission process per cluster in terms of a single parameter which accounts for the self-energy renormalization. It is shown that cluster antiresonances are responsible for the occurrence of a localization-delocalization transition which discriminates between insulating and conducting regimes for the electron transport. These results are interpreted in a general way on the basis of the scaling theory which involves the random phase approximation to characterize the behavior of the probability distribution connected to the transmittance. However, the scaling theory fails for particular values of the electron energy leading to singularities in the average transmittance called tips and dips. These singularities are related to the reminiscence of quantum interferences which the disorder is not sufficient to break.

DOI: 10.1103/PhysRevB.66.115322 PACS number(s): 71.23.−k, 71.30.+h, 73.23.Ad, 73.63.Nm

I. INTRODUCTION

The development of powerful microprocessors depends on continued progress in miniaturizing their components. The industry now manufactures devices with feature sizes below 180 nm, and, if current trends continue,[1] conventional silicon chips should reach their physical limits around 2012. Therefore, one of the challenges of technology is to find an alternative to silicon chips in order to control the electron transport at the nanometer or subnanometer scale.

At this length scale, the propagation of the electrons is said to be ballistic since their mean free path is much larger than the size of the device. As a result, scattering due to both impurities and phonons can be neglected and the transport, which must be treated quantum mechanically, can be described in terms of the transmission matrix formalism based on the Landauer-Buttiker theory.[2–4] Note that it has been shown recently that dissipation in small atomic wires can occur through phonon emission.[5] However, such a process takes place above a threshold voltage and will be neglected in the present work. The wave nature of the electron is responsible for the occurrence of quantum interferences, which were first observed for electron transport on mesoscopic length scales (see, for instance, Ref. 6). New phenomena connected to quantum interferences were discovered such as the weak localization, the universal conductance fluctuations, and the Aharonov-Bohm oscillations. The quantization of the conductance was observed in a nanowire obtained by drawing a metal constriction between the tip of a scanning tunneling microscope (STM) and a metal surface.[7,8]

In this context, well-controlled surfaces of solids are ideal templates for the formation of low-dimensional nanostructures with defined geometries.[9–11] The formation of two-dimensional monolayers on a perfect surface has now reached a high standard of understanding[12] and it is known that self-organized defects at the surface can be used to prepare nanodevices such as one-dimensional wires and confined two-dimensional structures.[13–15] Local probes such as STM, serve as acute tools to build nanostructures[16–20] and they can be used to excite the electronic and vibrational degrees of freedom of admolecules.[21]

Step decoration on vicinal surfaces can be exploited to obtain single high quality atomic chains and nanogratings depending on the growth scenario (namely, by changing temperature, deposition conditions, and terrace widths).[14,22] For the system Ag adsorbed on the vicinal Pt(997) surface (terrace width about 20 Å), it has been shown that, at $T > 200$ K, for a flux deposition about 10^{-4} atoms per second and a coverage around 0.2 ML, compact nanoscopic Ag clusters are quasiperiodically distributed along the Ag monatomic wires formed at the step bottoms.[23] These observations have motivated a theoretical study[24] to investigate the electronic transmission through a single rectangular cluster attached to an adsorbed nanowire. The cluster plays the role of a cavity for the electronic wave function leading to the occurrence of resonances and antiresonances, depending on the cluster size and shape. In particular, it has been demonstrated that a linear cluster can be used to switch the electronic current in the nanowire. The influence of a periodic distribution of linear clusters was recently investigated by Vasseur *et al.*[25] From the analysis of the electronic band structure, they showed that the band gaps can be opened near the Fermi energy as a result of both the periodic arrangement and the resonances induced by the clusters.

The present paper is devoted to a more general, and probably more physical, situation for which a set of linear clusters are quasiperiodically attached along the nanowire. We thus address the fundamental question of the influence of the disorder on the electronic transmission. The electronic transport properties in random lattices can be traced back to the seminal paper of Anderson[26] where the localization of quan-

tum states was first discussed. The so-called Anderson localization has been a central topic of intense researches during the last four decades (see, for instance, Ref. 27). By localization, it is meant that disorder, depending on the lattice dimensionality, can trap electrons by quantum interference to a finite region such that the conductor behaves as an insulator. In one-dimensional (1D) lattices, the original Anderson model was based on a single-band tight binding Hamiltonian for which the site energies were supposed to be random and independent. As a consequence, all the electronic states turned out to be localized, even if the disorder was infinitesimally small. However, it has been recently discovered that 1D lattices can support both discrete and continuum extended states when the disorder exhibits spatial correlations.[28–33]

In such 1D disordered lattices, the electronic transmittance (conductance) is a random variable which depends in a complicated manner on the disorder realization. Due to coherent interferences in the electron scattering from the static disorder, the transmission coefficient is not a self-averaging quantity. As a result, the statistical fluctuations of the transmittance grow faster than the average value, thus violating the central limit theorem. This apparently ill-posed problem was first solved by Anderson *et al.*[34] who introduced a general scaling theory to characterize the behavior of the probability distribution of the transmittance versus the lattice size. During the two later decades, the scaling theory of 1D lattice was developed in great details[35–39] and the full probability distribution of the transmittance was shown to obey a log-normal law which the typical value decreases exponentially with respect to the lattice size (for a recent review, see, for instance, Refs. 40, 41).

The paper is organized as follows. In Sec. II, we describe first the model and define the Hamiltonian used to characterize the electron transport. A decimation procedure allows us to renormalize the influence of the clusters and to describe the system as a strictly one-dimensional disordered lattice. The transfer matrix formalism is then used to reach the formal expression of the electronic transmittance. The numerical results are presented in Sec. III for a set of N identical linear clusters quasiperiodically arranged along the nanowire. Section IV is devoted to the interpretation of the electron transmittance with particular emphasis on the metallic-insulating transition and on the influence of quantum interferences depending on the disorder realization.

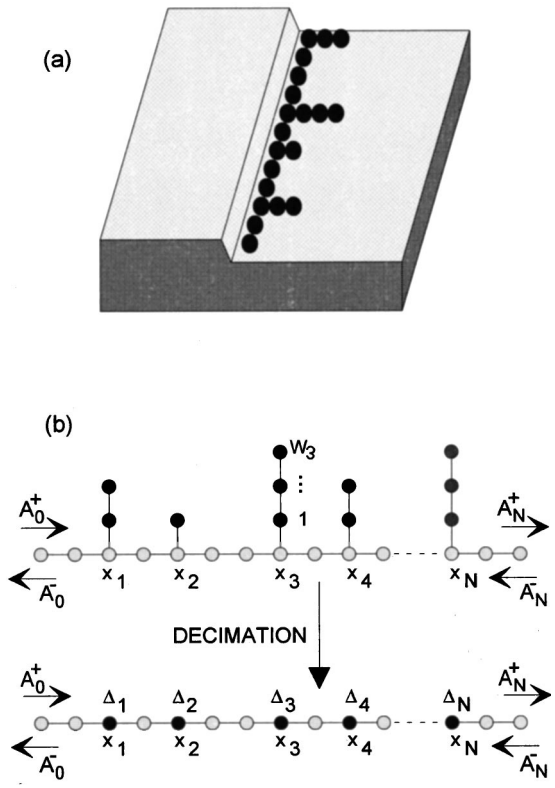

FIG. 1. (a) Schematic view of a monatomic nanowire formed by metal atoms (dark circles) decorating the step of a surface and containing a set of linear clusters of the same atomic species. (b) Schematic representation of the decimation procedure. x_j defines the position of the jth linear cluster and the arrows characterize the incident, the reflected and the transmitted electronic Bloch waves through the nanodevice.

II. THEORETICAL BACKGROUND

A. Model and Hamiltonian

Let us consider a set of metal atoms adsorbed on a terrace of a well-defined stepped surface within the growth conditions described in the Introduction [Fig. 1(a)]. Due to the singularity of the potential interaction, the adatoms are trapped in the preferential step sites and they form a perfectly ordered 1D lattice parallel to the step. The position of the atoms in the chain is described by a single index n and a denotes the lattice parameter [Fig. 1(b)]. Additional adatoms form a set of N clusters randomly attached to the nanowire. In this paper, we assume that the clusters have a simple linear shape. This assumption appears to be relevant from a qualitative point of view, since it is the simplest approach to discuss the influence of the cluster size and distribution on the electronic propagation along the nanowire. The disorder in the nanostructure is therefore due to both the quasiperiodicity of the distribution and the random size of these clusters. To describe the quasiperiodic distribution, let us define L as the average distance between two nearest neighbor clusters. It represents the distance associated to a periodic distribution, for which the clusters are located at their equilibrium positions $x_j^0 = jL$, where $j = 1,...,N$. The quasiperiodicity is taken into account by assuming that the positions x_j exhibit random fluctuations around their equilibrium values, namely, $x_j = x_j^0 + \delta_j a$, where $\{\delta_j\}$ denotes a set of N independent discrete random variables [Fig. 1(b)]. The randomness of the cluster size is taken into account by introducing a set of N random independent variables $\{W_j\}$, where W_j represents the random number of atoms in the jth cluster.

A model based on a single-electron scattering problem is used to study the quantum transport of electrons throughout this nanostructure. A single-band tight binding Hamiltonian describes the electron dynamics. The relevant parameters are the orbital energy and the hopping constant. When the atoms belonging to the nanowire are different from the atoms of the clusters, the nanowire and the clusters are characterized by

different sets of parameters. Let E_0 and J denote the orbital energy and the hopping constant between nearest neighbor sites, in the nanowire, respectively. In the same way, each cluster will be characterized by an orbital energy E_c and a hopping constant J_c, and, finally, J' will be connected to the hopping constant between the first atom of the jth cluster and the n_jth atom of the nanowire ($n_j = x_j/a$). The resulting Hamiltonian is thus written as

$$H = \sum_{\alpha} E_{\alpha} |\alpha\rangle\langle\alpha| + \sum_{\langle\alpha,\beta\rangle} J_{\alpha,\beta} |\alpha\rangle\langle\beta|, \tag{1}$$

where $\langle\alpha,\beta\rangle$ stands for a sum over the nearest neighbor sites only and $J_{\alpha,\beta}$ is equal to J, J_c, and J' depending on the nature of α and β (nanowire, clusters or mixed sites).

B. Clusters decimation procedure

To calculate the transmission coefficient of the electron in the nanowire through the attached clusters, we solve the Schrodinger equation related to the Hamiltonian H and seek wave functions in terms of Bloch waves that obey scattering boundary conditions as

$$\Psi_n = \begin{cases} A_0^+ e^{iqna} + A_0^- e^{-iqna}, & na > x_1, \\ A_N^+ e^{iqna} + A_N^- e^{-iqna}, & na > x_N. \end{cases} \tag{2}$$

In the region of the metallic nanowire located before the clusters ($na < x_1$), the wave function is a superimposition of incident and reflected Bloch waves with wave vectors q and amplitudes A_0^+ and A_0^-, respectively. The corresponding energy E_q is equal to the eigenenergy of the chain $E_q = E_0 + 2J\cos(qa)$. In the part of the metallic nanowire located after the set of clusters ($na > x_N$), the electron wave function is represented by a transmitted Bloch wave with amplitude A_N^+ and wave vector q, which propagates freely far apart from the clusters. This wave is also characterized by the energy E_q of the ideal chain. Note that, in order to generalize the notation, a backward Bloch wave with amplitude A_N^- is also introduced.

The relation connecting the different amplitudes is obtained by solving the Schrödinger equation $H|\Psi\rangle = E|\Psi\rangle$ for a given value $E = E_q$ of the energy. As detailed in Ref. 24, this equation can be expressed in an improved form by using a decimation procedure which allows us to eliminate the projected Schrodinger equations connected to the clusters and to locally renormalize the dynamical parameters describing the electron propagation. When it is applied to the jth cluster, the renormalization is responsible for the occurrence of a correction $\Delta_j(E)$ of the self-energy at the site where the jth cluster is linked to the nanowire, as

$$\Delta_j(E) = J'^2 \frac{P_{W_j-1}(E-E_c)}{P_{W_j}(E-E_c)}. \tag{3}$$

In Eq. (3), $P_W(X)$ represents the characteristic polynomial connected to the tight binding Hamiltonian of a cluster containing W sites. The polynomials of degrees 0 and 1 are defined as $P_0(X) = 1$ and $P_1(X) = X$, respectively, and the entire series can be generated by using the recursive relation

$$P_{m+1}(X) = XP_m(X) - J_c^2 P_{m-1}(X). \tag{4}$$

As shown in Ref. 24, the self-energy correction $\Delta_j(E)$ strongly depends on the incident energy. Indeed, it tends to infinity when the incident energy is equal to one of the eigenenergies of the jth cluster containing W_j atoms [i.e., $P_{W_j}(E-E_c) = 0$]. Such a feature, called resonance, leads to zero transmission. By contrast, antiresonances occur when the incident energy is equal to one of the eigenenergies of a finite size chain formed by the last $W_j - 1$ atoms belonging to the jth cluster [i.e., $P_{W_j-1}(E-E_c) = 0$]. In that case, the propagation along the nanowire through the jth cluster is not modified since the self-energy correction vanishes. Finally, by applying the decimation procedure to the set of N clusters, the scattering problem reduces to the transmission of an electronic wave function through an effective 1D disordered lattice containing N point defects characterized by self-energy corrections Δ_j [Fig. 1(b)].

C. Transfer matrix formalism

The determination of the electronic transmittance throughout this one-dimensional disordered lattice can be achieved by using the transfer matrix formalism. Within this formalism, the amplitudes $A_0^{\pm}$ and $A_N^{\pm}$ of the wave function in the regions free of defects are connected via the transfer matrix $M(N)$, as

$$\begin{pmatrix} A_N^+ \\ A_N^- \end{pmatrix} = M(N) \begin{pmatrix} A_0^+ \\ A_0^- \end{pmatrix}, \tag{5}$$

where the transfer matrix $M(N)$ is defined as

$$M(N) = \begin{pmatrix} 1/t^*(N) & \overline{r}(N)/\overline{t}(N) \\ -r(N)/\overline{t}(N) & 1/\overline{t}(N) \end{pmatrix}. \tag{6}$$

In Eq. (6), $t(N), r(N)$ and $\overline{t}(N), \overline{r}(N)$ stand for the left-to-right and right-to-left transmission and reflection coefficients of the N clusters, respectively, and t^* is the conjugate complex of t. These coefficients satisfy the well-known relation $|t(N)|^2 + |r(N)|^2 = |\overline{t}(N)|^2 + |\overline{r}(N)|^2 = 1$ which ensures the conservation of the probability current.

In our situation, the N clusters connect two identical media, i.e., the left- and right-hand side parts of the nanowire. As a result, the determinant of the transfer matrix is equal to one, leading to the relation $t(N) = \overline{t}(N)$. From the fundamental property of the transfer matrix method, i.e., the multiplicative composition rule, $M(N)$ is expressed as a product of N elementary transfer matrices M_j connected to the different clusters as

$$M(N) = M_N M_{N-1} \cdots M_2 M_1. \tag{7}$$

Since the connections between the clusters and the nanowire correspond to the sites $j = 1,...,N$, the interactions responsible for the scattering are coincident with the cluster positions along the wire, and the electronic wave function between

two clusters is a superimposition of progressive and regressive plane waves. Consequently, the elementary transfer matrix M_j at the jth defect site can be straightforwardly determined as

$$M_j=\frac{1}{t_j}\begin{pmatrix}\eta_j & \overline{r_j}\\ -r_j & 1\end{pmatrix}, \tag{8}$$

where the elementary reflection and transmission coefficients are expressed as

$$r_j=\frac{i\mu_j}{1-i\mu_j}e^{2iqx_j},$$

$$\overline{r_j}=\frac{i\mu_j}{1-i\mu_j}e^{-2iqx_j},$$

$$t_j=\frac{1}{1-i\mu_j},$$

$$\eta_j=\frac{t_j}{t_j^*}=\frac{1+i\mu_j}{1-i\mu_j}. \tag{9}$$

As shown in Eq. (9), these coefficients are characterized by a single parameter $\mu_j(E)=\Delta_j(E)/2J\sin(qa)$, which accounts for the energy dependence of the self-energy correction. In addition, a phase occurs in the elementary reflection coefficients which obeys to the symmetry of the scattering process ($\pm 2iqx_j$ according to the wave propagation is from left to right or from right to left).

Note that a direct calculation of the reflection and transmission coefficients $r(N)$ and $t(N)$ for the set of N clusters can be done by using the composition law [Eq. (7)]. These coefficients are expressed in terms of the elementary coefficients t_N, r_N and $\overline{r_N}$ as

$$t(N)=\frac{t_N t(N-1)}{1-r_N\overline{r}(N-1)},$$

$$\overline{r}(N)=\frac{\overline{r_N}+\eta_N\overline{r}(N-1)}{1-r_N\overline{r}(N-1)},$$

$$r(N)=\frac{r(N-1)+\eta(N-1)r_N}{1-r_N\overline{r}(N-1)} \tag{10}$$

with $\eta(N)=t(N)/t(N)^*$.

At this step, the electronic transmittance $T(N)=|t(N)|^2$ through the N clusters can be computed using either Eqs. (6)–(9) or Eq. (10). This transmittance is a random variable which depends on the realization of the disorder in two different ways. First, as shown in Eq. (9), the quasiperiodic nature of the cluster distribution leads to a random phase of the elementary reflection coefficients through the exponential term. Note that it does not modify the elementary transmission coefficient. Second, both the elementary reflection and transmission coefficients depend on the random nature of the cluster size through their dependence with respect to the μ_j parameters. In the present paper, we shall disregard this second effect and focus our attention on the first one, namely, the influence of the quasiperiodicity of the cluster distribution, only. Thus we shall assume that each cluster contains exactly the same number W of atoms and is characterized by the same parameter $\mu(E)$. The randomness in the cluster sizes will be studied in a forthcoming paper.

III. NUMERICAL RESULTS

The transmittance $T(N)$ through the N clusters is studied according to the disorder realization on the cluster distribution. The energy E of the incident Bloch wave is restricted to the allowed band of the chain, namely, $E_0-2|J|\leqslant E\leqslant E_0+2|J|$. Note that to reduce the number of parameters, we assume that the self-energies and hopping constants are the same everywhere, i.e., $E_c=E_0$ and $J_c=J'=J$. Such an assumption, although not strictly verified due to potential distortions in the neighborhood of steps and at the nanowire/cluster connections, should be quite valid when the nanowire and the clusters are formed by the same adspecies. In the reverse situation (i.e., when the chain and the clusters are constituted by different metallic species) new phenomena could occur, as studied in a forthcoming paper. The self-energy E_0 will be used as the origin of the energy ($E_0=0$), and the hopping constant J will be fixed equal to -1. To describe the quasiperiodicity of the cluster distribution we assume that each random variable δ_j can take the values 0, ± 1 with the same probability $p=1/3$. Such a choice qualitatively agrees with both the experimental[14] and theoretical[22,23] results where it has been shown that the position of the clusters exhibits weak fluctuations around the periodic configuration.

The transmittance for a periodic and a quasiperiodic lattice is compared in Fig. 2 for different values of the number N of clusters when their size and their average distance are equal to $W=2$ and $L=5a$, respectively. The full line represents the transmittance for the periodic configuration whereas the empty circles characterize the average value of the transmittance over the random fluctuations of the cluster positions. By increasing the number of clusters, a band structure emerges for the periodic lattice (full line), which depends on both the cluster size and the intercluster distance.[25] Quasiperfect bands are obtained when $N=50$. By contrast, the average transmittance for the quasi-periodic lattice (empty circles) decreases strongly as the number of clusters increases excepted at the center of the energy band where a single band remains around the antiresonance. This band is symmetric and the average transmittance is equal to one at the antiresonance, whatever the number of clusters. Its width strongly depends on the number N and it decreases as N increases. This behavior can be compared with the transmittance through a single cluster, which does not depend on the position of this cluster and exhibits a single wide antiresonance at the center of the energy band with two shoulders.[24]

The dependence of the previous features with respect to the number of atoms belonging to the clusters is illustrated in Fig. 3. When $W=3$ instead of 2, the transmittance through the perfectly periodic cluster lattice (full line) displays a band structure with, however, a reverse behavior since the center of the band corresponds to a forbidden band (reso-

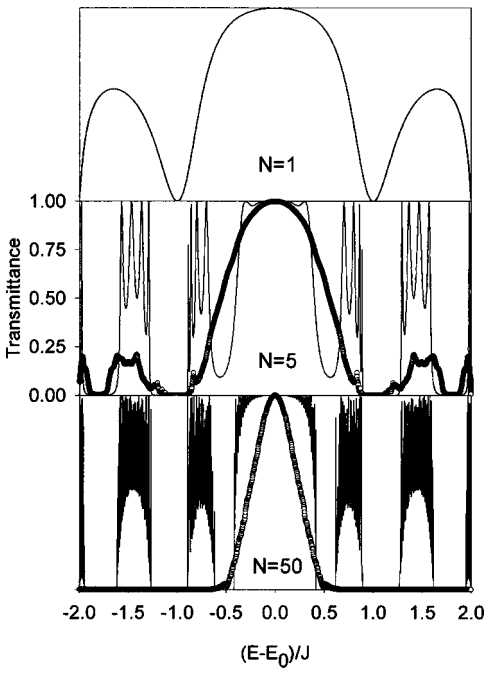

FIG. 2. Transmittance for a periodic and a quasiperiodic lattice when the cluster size and the average distance between clusters are equal to $W=2$ and $L=5$, respectively, for different values of the cluster number N. The full line represents the transmittance for the periodic configuration whereas the empty circles characterizes the average transmittance.

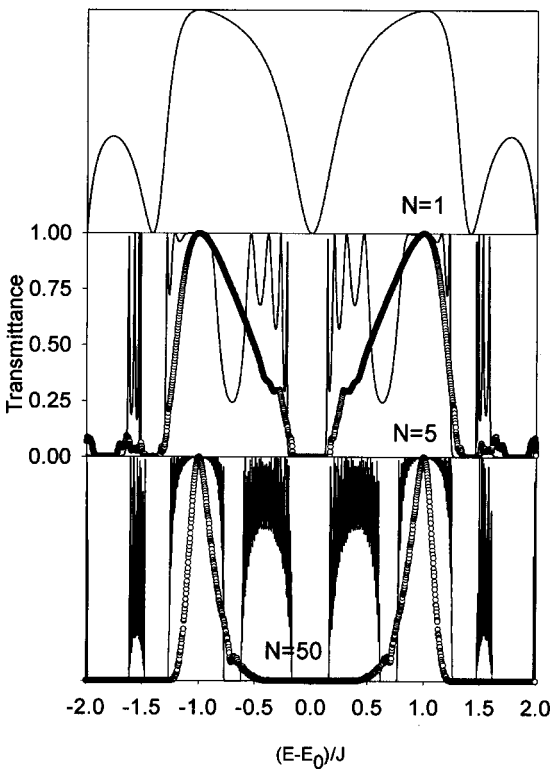

FIG. 3. Transmittance for a periodic and a quasiperiodic lattice when the cluster size and the average distance between clusters are equal to $W=3$ and $L=5$, respectively, for different values of the cluster number N. The full line represents the transmittance for the periodic configuration whereas the empty circles characterizes the average transmittance.

nance) instead of an allowed band (antiresonance). Such a result is consistent with the conditions imposed by $\Delta(E)$ according to W is even or odd. The average transmittance for the quasiperiodic lattice (empty circles) decreases when N increases. It is mainly characterized by two broad bands centered around the antiresonances and symmetrically located around the band center. As in the previous situation, the two bands narrow as N increases without appreciably changing their position. The average transmittance is equal to one at the antiresonances. Note that the profile of the bands is rather asymmetric, in marked contrast with the previous situation. It can be compared with the behavior of the transmittance through a single cluster which exhibits two antiresonances located at the energies $E=E_0\pm J$.[24]

In Figs. 4, the average [full line in Fig. 4(a)] and standard deviation [full line in Fig. 4(b)] of the transmittance are shown when the cluster size, the average distance between nearest neighbor clusters and the cluster number are equal to $W=2$, $L=10a$, and $N=70$, respectively. The average transmittance shows a symmetric, single band located at the antiresonance ($E=0$). Although the curve varies in a quasicontinuous way with respect to the energy, it exhibits two tips which are symmetrically located on both sides of the antiresonance, and which occur for discrete values of the energy equal to $E_{\rm tip}=E_0\pm 0.28J$. These tips characterize a local increase of the average transmittance for a given value of the electron energy. The values of the energy at which these tips occur do not depend on the number N of clusters, but they are shifted when the average distance L between the clusters is changed. More precisely, the tip energy moves away from the antiresonance maximum as L decreases. The standard deviation is very small around the maximum of the transmittance, but it increases in a dramatic way to become larger than the average value when the energy shifts away from the antiresonance. As a result, it exhibits two symmetrically located maxima.

Another configuration is shown in Fig. 5 when $W=2$, $L=16a$, and $N=30$, i.e., by increasing the intercluster distance L and decreasing the number N of clusters. Both the average transmittance [full line in Fig. 5(a)] and the standard deviation [full line in Fig. 5(b)] exhibit a similar behavior as in the previous configuration. However, in marked contrast with the previous case, the average transmittance shows four tips at the energies $E_{\rm tip}=E_0\pm 0.18J$ and $E'_{\rm tip}=E_0\pm 0.53J$ and two dips, corresponding to a local decrease of the average transmittance, at the energies $E_{\rm dip}=E_0\pm 0.36J$.

The behavior of the probability distribution of the transmittance is shown in Fig. 6 when the cluster size, the averaged distance between nearest neighbor clusters and the cluster number are equal to $W=2$, $L=10$, and $N=70$, respectively (see Fig. 4). The various figures represent the probability distribution for distinct values of the incident energy, i.e., for different values of the average transmittance. The shape of this probability distribution evolves continuously with respect to the incident energy and it appears to be a slowly varying function of the transmittance excepted when a ''tip'' or a ''dip'' region is reached. We see that when the average

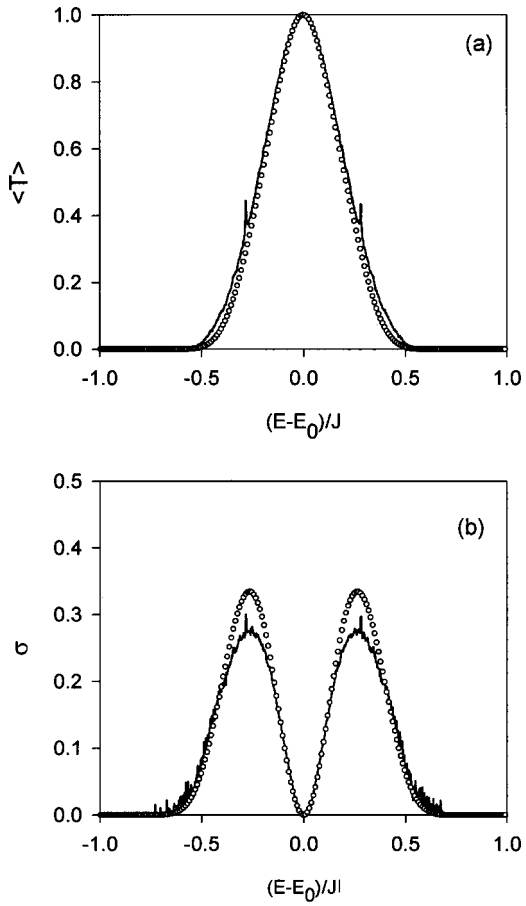

FIG. 4. (a) Average value of the transmittance (full curve) when $W=2$, $L=10$, and $N=70$. The empty circles represent the theoretical curve obtained by using the scaling theory [see Eq. (15) in Sec. IV B]. (b) Standard deviation of the transmittance (full curve) when $W=2$, $L=10$, and $N=70$. The empty circles represent the theoretical curves [see Eq. (15) in Sec. IV B].

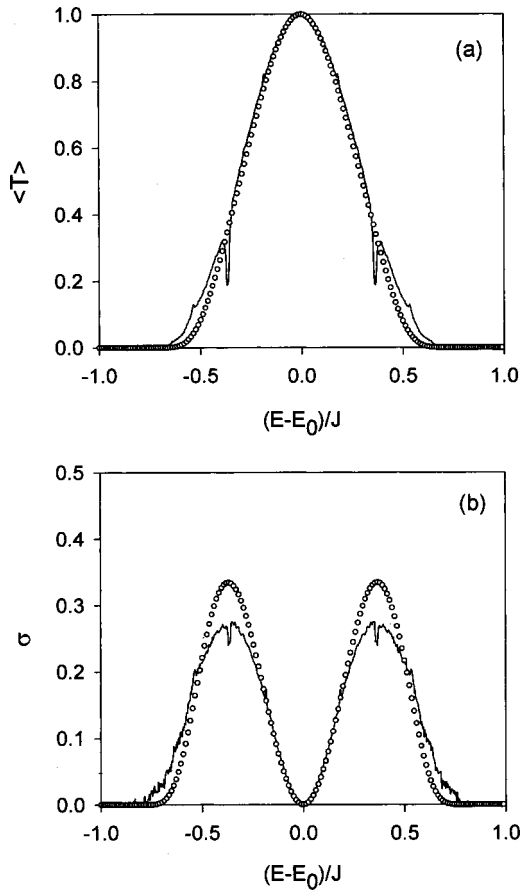

FIG. 5. (a) Average value of the transmittance (full curve) when $W=2$, $L=16$, and $N=30$. The empty circles represent the theoretical curve obtained by using the scaling theory [see Eq. (15) in Sec. IV B]. (b) Standard deviation of the transmittance (full curve) when $W=2$, $L=10$ and $N=70$. The empty circles represent the theoretical curve [see Eq. (15) in Sec. IV B].

transmittance is close to 1, i.e., when the incident energy of the electron is close to the anti-resonance, the probability distribution behaves as an exponential law which reaches its maximum for $T=1.0$ [Fig. 6(a)]. As the energy shifts away from the antiresonance [Figs. 6(b) and 6(c)], the distribution loses its local character and reaches a quasiuniform shape for $\langle T\rangle=0.5$ with only a small dip at $T=0$. As the average transmittance goes slightly below 0.5, the probability distribution displays a fully different behavior since it tends to a log-normal distribution which becomes maximum for $T=0$ [Figs. 6(f) and 6(g)]. For an average transmittance equal to $\langle T\rangle=0.45$ [Fig. 6(e)], which corresponds to the occurrence of a tip, the behavior is totally different since the distribution exhibits a set of exponential decaying profiles. This distribution seems to condensate around discrete values which are more and more concentrated when the transmittance values become closer and closer to zero. Similar results would be obtained (not shown) for values of W, L, and N corresponding to Fig. 5, with the occurrence of singular distribution profiles at each tip and dip of the transmittance curve.

IV. INTERPRETATION AND DISCUSSION

A. Localization-delocalization transition. Singularity of the localization length

The present numerical results appear to be in marked contrast with the well-known Anderson problem, for which no transition should occur in a one-dimensional lattice. Indeed, they point out that a one-dimensional nanowire containing randomly distributed clusters exhibits a localization-delocalization transition which depends on the incident energy of the electron propagating through the quasiperiodic cluster distribution. Such a transition occurs when the incident energy of the electron coincides with the antiresonances of a cluster. At these antiresonances, the self-energy correction $\Delta(E)$ vanishes. When all the clusters are identical (same shape and size) their self-energy correction is the same, and the electron propagates freely. The transmittance is thus strictly equal to one whatever the number and the position of these clusters. Note that a similar effect was previously predicted by Denbigh and Rivier[42] in a slightly different system. Indeed, the authors have shown that the Schrödinger equation connected to a Kronig-Penney potential with identical rectangular barriers randomly spaced exhibits an infinite set of extended eigenstates.

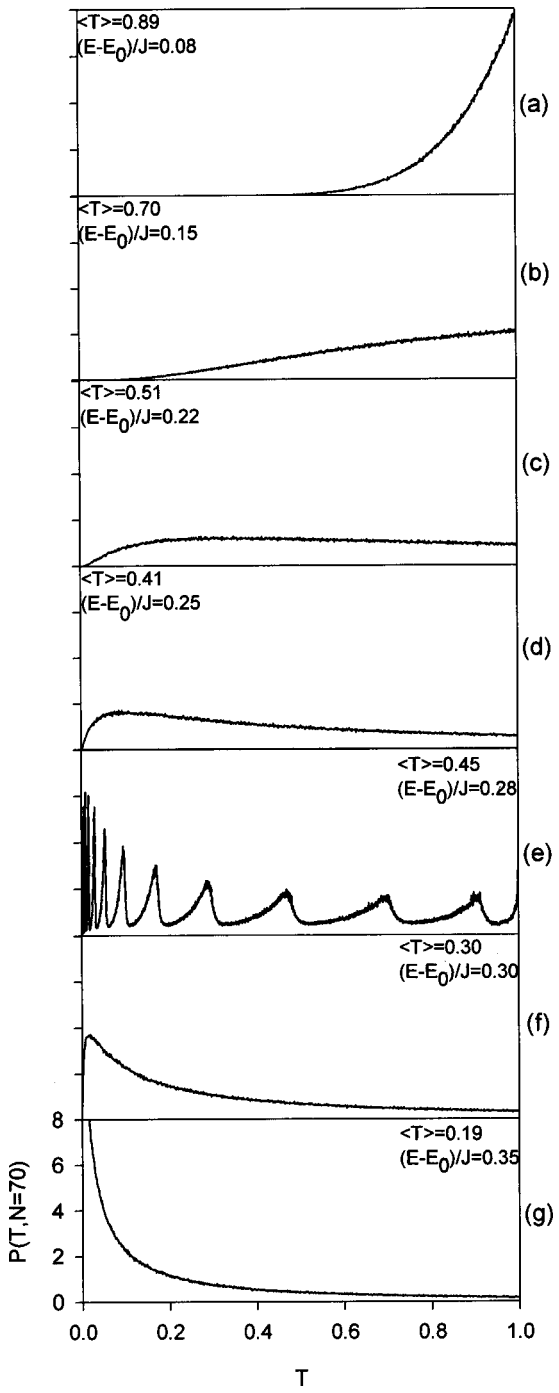

FIG. 6. Probability distribution of the transmittance when $W=2$, $L=10$, and $N=70$ for different values of the incident energy of electron (i.e., for different values of the average transmittance). Both the X and Y axis are the same for the different graphs.

The relevant parameter characterizing the transition is the localization length ξ. To determine its expression, we take advantage of the fact that, in the close neighborhood of an antiresonance, the elementary reflection coefficients are very small and the composition law for the transmission coefficients [Eq. (10)] reduces to a strictly multiplicative law. Since the randomness of the cluster locations does not modify the elementary transmission coefficients, it is straightforward to show that the transmittance behaves as $T(N)\approx\exp(-N\mu^2)$. The localization length is thus defined as

$$\xi(E)=\frac{2L}{\mu^2}=\frac{8LJ^2\sin^2(qa)}{\Delta(E)^2}. \tag{11}$$

When the energy approaches an anti-resonance, the self energy correction $\Delta(E)$ tends to zero leading to a dramatic increase of the localization length, which diverges at the antiresonance. As shown in Ref. 24, the self-energy correction behaves as $\Delta(E)\sim E-E_A$ when the energy E is close to an antiresonance with energy E_A. As a consequence, the localization length exhibits a power law dependence with respect to the energy, i.e., $\xi(E)\sim|E-E_A|^{-\nu}$ in which the divergence is controlled by the critical exponent $\nu=2$. Equation (11) is equivalent to the expression of the localization length occurring in the one-dimensional Anderson problem within the weak disorder limit. For a complete comparison with the Anderson problem, note that the self-energy correction plays the role of the standard deviation of the one-site random energies and that the cluster antiresonances correspond to the situation for which the fluctuations of the one-site energies vanish. Note that, strictly speaking, the localized or extended nature of the electronic state is an intrinsic property of an infinite one-dimensional lattice. However, as it will be shown in the following section, a state will be denoted localized (or extended) when the corresponding localization length is smaller (or greater) than the size of the nanowire.

B. Random phase approximation and scaling theory

The occurrence of a localization-delocalization transition allows us to distinguish between two different regimes for the electronic transport. Such a transition, which does not occur for a strictly one-dimensional disordered lattice, has nevertheless been observed in quasi-one-dimensional wires and interpreted within the framework of the scaling theory.[34–41] Within this theory, the probability distribution of the transmittance approaches a universal function which depends only on a limited number of parameters characteristic of the system. It can be determined by taking advantage of the formal resemblance between the random evolution of the transmittance $T(N)$ versus the number N of clusters and the time evolution of a stochastic variable $X(t)$, N playing the role of the time t. In fact, such a procedure can be straightforwardly exploited by using the resistance $\rho(N)=[1-T(N)]/T(N)$ instead of the transmittance $T(N)$, as the relevant variable. In this context, the evolution of the probability distribution $P(\rho,N)$ is given by a Fokker-Planck equation expressed as

$$\frac{\partial P(\rho,\tau)}{\partial\tau}=\frac{\partial}{\partial\rho}\left[(\rho+\rho^2)\frac{\partial P(\rho,\tau)}{\partial\rho}\right], \tag{12}$$

where $\tau=N\mu(E)^2=2NL/\xi(E)$. To obtain this equation, it is assumed that the cumulative phase of the reflexion coefficient $r(N)$ behaves as a random variable uniformly distributed between 0 and 2π, and the random phase approximation is applied. Two limit cases can be considered depending on

the typical value of the resistance. For small values of the resistance ($\rho^2 \ll \rho$), the transmittance is close to one and the solution of Eq. (12) yields an exponential distribution expressed as

$$P(\rho,\tau)=\frac{1}{\tau}\exp\left(-\frac{\rho}{\tau}\right). \tag{13}$$

For large values of the resistance ($\rho^2 \gg \rho$), the transmittance is close to zero and the solution of Eq. (12) has the form of a log-normal distribution:

$$P(\rho,\tau)=\frac{1}{\rho\sqrt{4\pi\tau}}\exp\left(-\frac{[\ln(\rho)-\tau]^2}{4\tau}\right). \tag{14}$$

These results perfectly agree with the observed behavior of the probability distribution of the transmittance drawn in Fig. 6. They show that the electronic transport along the nanowire with randomly attached clusters evolves according to two distinct scaling regimes in a way similar to the quasi one-dimensional wire, depending on the ratio NL/ξ between the lattice size NL and the localization length $\xi(E)$. When $NL/\xi \ll 1$, the regime is said to be metallic (or delocalized) and the average transmittance decreases linearly with the size NL, according to the law $\langle T(N)\rangle = 1-2NL/\xi(E)$. The fluctuations of the transmittance around its average value remain small and the average value is physically relevant. By contrast when $NL/\xi \gg 1$, the fluctuations become greater than the average transmittance. The typical transmittance exhibits an exponential decrease versus NL as $T_t(N)=\exp(-2NL/\xi)$ and the regime is said to be insulating (or localized).

Approximate expressions for the average transmittance $\langle T(N)\rangle$ and its second moment $\langle T(N)^2\rangle$ can be determined self-consistently (see Appendix A). They are given as

$$\langle T(N)^\alpha\rangle=\left(\frac{2e^{2NL/\xi}}{3-e^{-4NL/\xi}}\right)^{\alpha^2/3} e^{-2\alpha NL/\xi} \tag{15}$$

with $\alpha=1, 2$. In Figs. 4(a) and 5(a), the empty circles represent the behavior of the theoretical average transmittance obtained by using Eq. (15). In the same way, the empty circles in Figs. 4(b) and 5(b) characterize the evolution of the theoretical standard deviation of the transmittance ($\sigma = \sqrt{\langle T^2\rangle - \langle T\rangle^2}$).

These theoretical curves perfectly reproduce the numerical results in the neighborhood of the antiresonance for which the average transmittance is significant, i.e., in the metallic regime. Equation (15) leads to a linear decrease of both the averaged transmittance and its second moment, $\langle T(N)^\alpha\rangle = 1-2\alpha NL/\xi$. In addition, the relative standard deviation of the transmittance remains weak and scales as $\delta T/\langle T\rangle \approx 2NL/\xi$, in very good agreement with the scaling theory. However, an energy shift from the antiresonance maximum leads to a loss of accuracy with numerical data although the results still remain qualitatively correct. Note, in particular, that Eq. (15) shows an exponential decrease of both the average transmittance and its second moment as $\langle T(N)^\alpha\rangle = \exp(-4NL/3\xi)$. In marked contrast with the metallic regime, the relative standard deviation increases in an exponential way as $\delta T/\langle T\rangle \approx \exp(2NL/3\xi)$ which accounts for the large distribution law of the transmittance in the insulating regime.

C. Weak disorder limit

Although the scaling theory interprets most of the numerical results, it cannot explain the occurrence of the tips and dips in the average transmittance. The main reason is that the tips and dips occur at energies for which the random phase approximation does not apply to build the Fokker-Planck equation [Eq. (12)]. To discuss this phenomenon more precisely, let us consider the weak disorder limit to study the behavior of the transmittance, especially in the neighborhood of an antiresonance. Indeed, tips and dips can a priori occur everywhere in the average transmittance curve, as shown in Figs. 4 and 5. However, interpreting their occurrence in the antiresonance neighborhood is analytically easier and leads to the understanding of the physical phenomena. We thus assume that the self-energy correction $\Delta(E)$ is a small parameter and perform a second order perturbative theory to determine the transmittance. From the composition law [Eq. (10)], the transmission coefficient is expressed as

$$t(N)=t_N t_{N-1}\cdots t_1 \exp\left[-\sum_{i=1}^{N-1}\ln[1-r_{i+1}\overline{r}(i)]\right]. \tag{16}$$

When $\Delta(E) \ll 1$, the composition law for the right-to-left reflexion coefficients reduces to an additive law. Therefore, by considering the second order perturbation theory of Eq. (16) with respect to $\Delta(E)$, the transmission coefficient through N identical clusters can be expressed in an improved form as

$$t(N)\approx t_1^N \exp\left[\sum_{i=1}^{N-1}\sum_{j=1}^{i} r_{i+1}\overline{r_j}\right]. \tag{17}$$

At this step, by using Eq. (9), the transmittance is finally expressed as

$$T(N)\approx\exp[-S(N)], \tag{18}$$

where the quantity $S(N)$ is defined as

$$S(N)=\mu^2\left|\sum_{j=1}^{N} e^{2iqx_j}\right|^2. \tag{19}$$

From a physical point of view, the quantity $S(N)$ measures the (second order) quantum probability to observe the electron in the left-hand side of the nanowire after it has been scattered by the set of N clusters. It appears as the square modulus of the probability amplitude for the realization of the process and takes into account for the probability for the electron to be scattered by every cluster and for the quantum interferences between two different paths involving the interaction with two distinct clusters.

These interferences play a crucial role to understand the behavior of $T(N)$. Indeed, when the clusters are periodically distributed along the nanowire ($\delta_j=0$), the quantum probability $S(N)$ exhibits a particular behavior when the incident wave vector is quantized according to the relation $q=m\pi/2L$, where m denotes an integer. For even values of m, the different paths give rise to constructive interferences leading to a maximum probability $S(N)$ equal to μ^2N^2. The corresponding value of the transmittance is small since the wave vector lies in the forbidden bands induced by the periodic distribution of the clusters. For odd values of m, two paths involving two successive clusters interfere destructively leading to a minimum value of $S(N)$ equal to zero for even N values and to μ^2 for odd N values. Since μ is assumed to be small, the corresponding transmittance in Eq. (18) is maximum whatever N.

When the clusters are quasiperiodically distributed, the quantum probability $S(N)$ becomes a random variable which strongly depends on the disorder realization in the cluster positions. The behavior of this probability is thus the result of the influence of the randomness on the quantum interferences. Its characterization can be performed by taking advantage of its formal resemblance with a two-dimensional Brownian trajectory. Indeed, $S(N)$ can be formally expressed as $S(N)=|X(N)+iY(N)|^2$ where the two random variables $X(N)$ and $Y(N)$ are defined as

$$X(N)=\mu\sum_{j=1}^{N}\cos(2qx_j),$$

$$Y(N)=\mu\sum_{j=1}^{N}\sin(2qx_j). \tag{20}$$

From Eq. (20), $S(N)$ can be identified with the square modulus of the distance performed by a Brownian particle with coordinates $X(N)$ and $Y(N)$ along a two-dimensional trajectory. The number N plays the role of the time. The evolution of $S(N)$ strongly depends on the values of the incident wave vector and three distinct behaviors appear which correspond to three different kinds of Brownian motions.

When the wave vector is different from $m\pi/2L$, the Brownian particle describes a continuous and isotropic two-dimensional trajectory [Fig. 7(a)]. The successive jumps realized by the particle are random and independent and the random phase approximation can be applied. The evolution of the probability distribution $g(S,N)$ is described by the well-known two-dimensional diffusion equation. Its solution is a universal exponential function $g(S,\tau)=\exp(-S/\tau)/\tau$. As a result, it is straightforward to show that the probability distribution for the transmittance is expressed as

$$P(T,N)=\frac{\xi}{2NL}T^{\xi/2NL-1}, \tag{21}$$

where ξ is the localization length defined in Eq. (11). Although the probability distribution in Eq. (21) is obtained by assuming that the self-energy correction remains a small parameter, we can qualitatively interpret the transition between the metallic and insulating regimes. Indeed, this distribution shows a power law with respect to the transmittance which depends on the sign of the exponent $\xi/2NL-1$. When the exponent is positive ($2NL<\xi$), the distribution is maximum when the transmittance is close to one and characterizes the metallic regime. By contrast, when the exponent is negative ($2NL>\xi$), the distribution turns out to be maximum when the transmittance is close to zero and it corresponds to the insulating regime. Note that Eq. (21) leads to a crossover between the two regimes which occurs when $\langle T(N)\rangle=0.5$. In this case we obtain a uniform distribution, in very good agreement with the numerical results (Fig. 6).

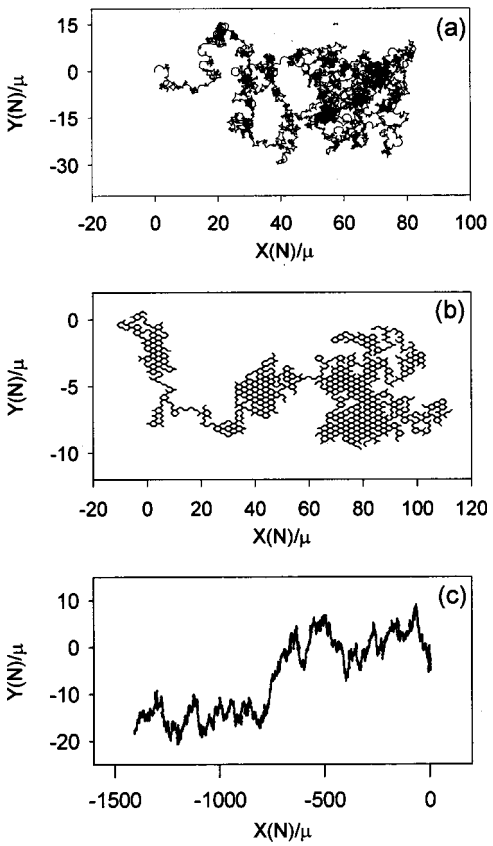

FIG. 7. Two-dimensional Brownian motion associated to the evolution of the quantum probability $S(N)$. (a) $q\neq m\pi/2L$, (b) $q=m\pi/2L$, with m odd, and (c) $q=m\pi/2L$, with m even.

When the incident wave vector is equal to $m\pi/2L$, the probability distributions of both the quantum probability $S(N)$ and the transmittance $T(N)$ suddenly behave in a drastically different way. In that case, the random phase approximation is not valid and an exact calculation is required to determine the probability distribution of $S(N)$. In Appendix B, it is demonstrated that $S(N)$ becomes a discrete random variable and its possible values depend on the parity of both m and N. In other words, the continuous trajectory of the Brownian particle turns out to be discrete since the particle is constrained to move on a two-dimensional lattice. The shape of the unit cell of this lattice depends on the value of the wave vector q. The probability distribution connected to $S(N)$ is thus defined as (Appendix B)

$$g(S,N)=\frac{1}{3^{N_1+N_2}}\sum_{r_1=0}^{N_1}\sum_{s_1=0}^{N_1-r_1}\sum_{r_2=0}^{N_2}\sum_{s_2=0}^{N_2-r_2}\frac{N_1!N_2!\,\delta[S-S(r_1,s_1,N_1,r_2,s_2,N_2)]}{r_1!s_1!(N_1-r_1-s_1)!r_2!s_2!(N_2-r_2-s_2)!}, \tag{22}$$

where the possible values of $S(N)$ are expressed as

$$\begin{aligned}S(r_1,s_1,N_1,r_2,s_2,N)/\mu^2=&\{[1-\cos(m\pi a/L)](r_1-r_2)\\&+\cos(m\pi a/L)(N_1-N_2)\}^2\\&+\{[2(s_1-s_2)+r_1-r_2-N_1\\&+N_2]\sin(m\pi a/L)\}^2.\end{aligned} \tag{23}$$

As shown in Appendix B, the values of the integer numbers N_1 and N_2 depend on both m and N. The behavior of the distribution $g(S,N)$ is illustrated in Fig. 8 when the cluster size, the average distance between nearest neighbor clusters and the cluster number are equal to $W=2$, $L=16$, and $N=30$, respectively. When the integer m is odd [$m=15$ in Fig. 8(a)], the corresponding values of N_1 and N_2 are $N_1=N_2=N/2$ when N is even and $N_1=(N-1)/2$, $N_2=(N+1)/2$ when N is odd. The probability $g(S,N)dS$ exhibits a set of exponential decaying bar spectrum distributed according to a Gaussian envelop. Note that, as shown in the inset, this result perfectly agrees with the numerical data obtained within the transfer matrix formalism. The most probable value of the transmittance is localized in the very close neighborhood of the origin $S=0$. Therefore, the typical value for the transmittance is close to 1 which is thus associated to the occurrence of a tip in the average transmittance. The Brownian character of the motion of the particle remains but it appears to be slightly anisotropic. In addition, the particle is constrained to move on a two-dimensional lattice which is responsible for the discretization of the possible values of the random variable $S(N)$ [Fig. 7(b)]. When the integer m is even [$m=14$ in Fig. 8(b)], the corresponding values of N_1 and N_2 are $N_1=N$ and $N_2=0$. As previously obtained, the probability $g(S,N)dS$ exhibits a set of exponential decaying bar spectrum with a Gaussian envelop. The most probable value of $S(N)$ is approximately equal to $S_t=\mu^2N^2[1+2\cos(m\pi a/L)]^2/9$. As a result, the typical transmittance $T_t=\exp(-S_t)$ is very small and a dip occurs in the average transmittance. In other words, a drift motion is added to the random walk performed by the Brownian particle which thus moves far away from its starting position. The distance covered by the particle scales as N leading to an increase of the quantum probability which behaves as N^2 [Fig. 7(c)]. Although these results are in qualitative agreement with the numerical data represented in the inset, they point out the limitation of the theory which remains valid in the neighborhood of the antiresonance, only. Especially, the theoretical distribution tends to spread out over larger $S(N)$ values than the numerical one.

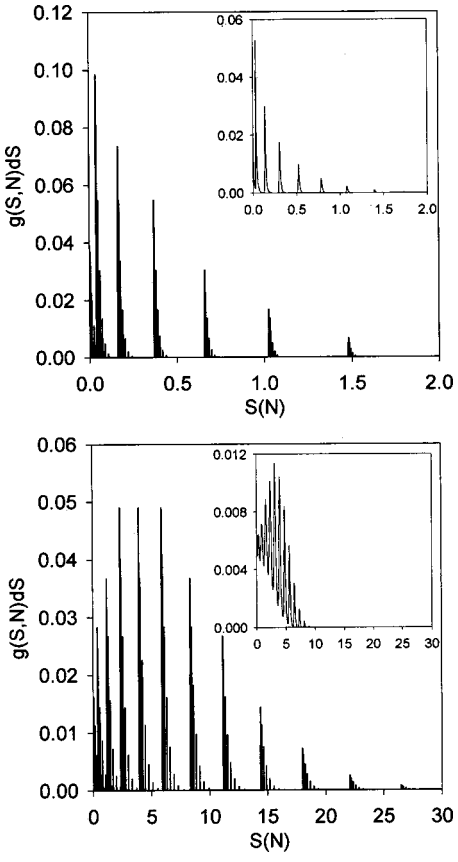

FIG. 8. Theoretical probability distribution of the quantum probability $S(N)$ when $W=2$, $L=16$, and $N=30$. (a) Incident wave vector $q=(L-1)\pi/2L$. (b) Incident wave vector $q=(L-2)\pi/2L$. The insets represent the corresponding numerical results obtained within the transfer matrix formalism.

This singular behavior of the probability distribution of $S(N)$ is responsible for the observed features shown in Figs. 4, 5, and 6(e). Indeed, the discretization of the quantum probability $S(N)$ when $q=m\pi/2L$ leads to the discrete behavior of the random transmittance and thus to the observed condensation of its probability distribution. In addition, the previous analysis allows us to evaluate the theoretical energies of both the tips and the dips. Indeed, when $W=2$, $L=16$, and $N=30$ (Fig. 5), the theoretical results lead to $E_{\rm tip}=E_0\pm0.19J$ and $E'_{\rm tip}=E_0\pm0.58J$ which compare very well with the numerical results $E_{\rm tip}=E_0\pm0.18J$ and $E'_{\rm tip}=E_0\pm0.53J$, respectively (see Sec. IV). In the same way, the predicted dip is equal to $E_{\rm dip}=E_0\pm0.36J$ in good agreement with the numerical values equal to $E_{\rm dip}=E_0\pm0.39J$. When $W=2$, $L=10$ and $N=70$, the theoretical tip energies are equal $E_{\rm tip}=E_0\pm0.31J$, in nice agreement with the numerical value equal to $E_{\rm tip}=E_0\pm0.28J$.

V. CONCLUSION

In this paper, the electronic transmission through a set of metallic linear clusters randomly distributed along an adsorbed nanowire has been investigated by using a single

band tight-binding Hamiltonian. It has been shown that the extended nature of the clusters forming a lattice along the nanowire is responsible for the occurrence of a localization-delocalization transition when the incident energy of the electron coincides with the cluster antiresonances. This transition, which is similar to the localization-delocalization transition occurring in a quasi-one-dimensional wire, has been interpreted in terms of the scaling theory. Two different regimes are found for the electronic transport depending, on the ratio between the localization length ξ and the lattice size. In the very close neighborhood of an antiresonance, the regime is metallic and corresponds to a localization length greater than the lattice size. In other words, ξ is larger than the size of the cluster device along the atomic chain. By contrast, when the energy shifts away from the antiresonance, the electron localization takes place and an insulating regime is established.

We have shown that the scaling theory, based on the random phase approximation, fails for particular values of the incident energy. Indeed, tips and dips occur in the curve of the average transmittance vs the energy for discrete values of the energy. In these tip or dip regions, the probability distribution of the transmittance exhibits a singular behavior which is interpreted within the weak disorder approximation. Basically, outside the tip and dip regions, the disordered nature of the cluster distribution is responsible for the breaking of the coherence in the electron propagation. No quantum interference occurs and the transmittance behaves as a continuous, random variable distributed according to a universal function which depends on the number of clusters, only. By contrast, in the tip or dip regions, the disorder is not sufficient to eliminate the influence of the quantum interferences and the transmittance becomes a discrete, random variable. The tips correspond to a situation for which the typical value of the quantum probability to observe the electron in the region located before the clusters is minimum while the dips characterize the memory of the forbidden bands and correspond to a situation for which the typical value of the quantum probability is maximum.

To conclude, let us discuss the implications of the previous results in the electronic transport at the nanometer scale. As pointed out in Ref. 24, the attachment of reduced size atomic clusters along a nanowire could open a new way for fabricating nanodevices with specific functionalities, able to mimic the operations realized by integrated circuits (current switching, transistor effect, logical gates, ...). The main idea is to obtain the desired functionalities by controlling the quantum interferences experienced by the electron wave function. However, the disordered nature of such real nanodevices cannot be disregarded since the disorder can have a dramatic influence on the electronic transport by breaking the quantum coherence and, thus, preventing the efficiency of the desired functionalities. Our results show that this is no longer the case when the disorder is responsible for small fluctuations of the cluster positions around the periodic distribution, only. In that case, the disorder destroys the coherence created by the periodicity and the transmittance is essentially governed by the single cluster antiresonances. The width of the allowed bands can be controlled by changing the lattice size since it decreases as the cluster number N increases and scales as $1/\sqrt{N}$.

Note that the present study has pointed out some specificities of such nanodevices within a model limited to identical, linear clusters attached to a nanowire formed by the same atomic species. Further developments are required to study, on one hand, the influence of the shape and size of the clusters on the electron conductance and, on the other hand, the modifications induced when two different metal species for the wire and the clusters are considered.

APPENDIX A: EXPRESSION OF $\langle T^{\alpha}\rangle$

From the relation between the resistance and the transmittance, the αth moment of $T(N)$ can be written as

$$\langle T(N)^{\alpha}\rangle = \langle \exp\{-\alpha \ln[1+\rho(N)]\}\rangle \tag{A1}$$

Instead of performing a cumulant expansion of the averaged value of the exponential, we introduce a trial function $u(\tau)$ from the following identification:

$$\langle T^{\alpha}\rangle = \exp\left[-\alpha\langle \ln(1+\rho)\rangle + \frac{\alpha^2}{2}u(\tau)\right]. \tag{A2}$$

This trial function is determined self-consistently by using the Fokker-Planck equation [Eq. (12)]. Indeed, it is straightforward to show that $\langle \ln(1+\rho)\rangle = \tau$. Moreover, both $\langle T\rangle$ and $\langle T^2\rangle$ are not independent and satisfy the equation

$$\frac{d\langle T\rangle}{d\tau} = -\langle T^2\rangle. \tag{A3}$$

By using Eq. (A3) to determine $u(\tau)$, we find that it verifies the first order nonlinear differential equation

$$\frac{1}{2}\frac{du}{d\tau} + \exp\left(-\tau + \frac{3}{2}u\right) = 1. \tag{A4}$$

Equation (A4) reduces to a Bernoulli equation which can be exactly solved leading to

$$u(\tau) = \frac{2}{3}\ln\left(\frac{2e^{\tau}}{3-e^{-2\tau}}\right). \tag{A5}$$

By inserting Eq. (A5) into Eq. (A2), we obtain the resulting expressions of $\langle T\rangle$ and $\langle T^2\rangle$ in Eq. (15).

APPENDIX B: CALCULATION OF THE DISTRIBUTION OF THE QUANTUM PROBABILITY $S(N)$

Instead of directly studying the probability distribution connected to $S(N)$, let us focus on the two-dimensional probability distribution $h(X,Y)$. Since the variables X and Y depend on the set of the N independent random variables $\{\delta_j\}$ defined in Sec. II, the function $h(X,Y)$ can be easily determined as products of Dirac functions as

$$h(X,Y)=\frac{1}{3^N}\sum_{\delta_1=-1}^{+1}\cdots\sum_{\delta_N=-1}^{+1}\delta\left(X-\mu\sum_{j=1}^{N}\cos(2qx_j)\right)\times\delta\left(Y-\mu\sum_{j=1}^{N}\sin(2qx_j)\right). \quad \text{(B1)}$$

By Fourier transforming Eq. (B1), the characteristic function $\Phi(U,V)$ connected to the distribution function $h(X,Y)$ is defined as

$$\Phi(U,V)=\prod_{j=1}^{N}\langle e^{iU\mu\cos(2qx_j)}e^{iV\mu\sin(2qx_j)}\rangle. \quad \text{(B2)}$$

When the incident wave vector is equal to $q=m\pi/2L$, an analytical expression of the characteristic function $\Phi(U,V)$ can be determined. Indeed, in that case, we have

$$\cos(2qx_j)=(-1)^{jm}\cos(2qa\delta_j),$$
$$\sin(2qx_j)=(-1)^{jm}\sin(2qa\delta_j). \quad \text{(B3)}$$

Therefore, three situations occur depending on the parity of both m and N. For even m values, $(-1)^{jm}=1$ whatever j. As a result, the characteristic function $\Phi(U,V)$ factorizes as the product of N identical and independent terms as

$$\Phi(U,V)=\prod_{j=1}^{N}\langle e^{iU\mu\cos(2qa\delta_j)}e^{iV\mu\sin(2qa\delta_j)}\rangle \equiv\langle e^{iU\mu\cos(2qa\delta_j)}e^{iV\mu\sin(2qa\delta_j)}\rangle^N. \quad \text{(B4)}$$

For odd m values, a different factorization occurs which involves the parity of the cluster number N. However, instead of performing the calculation for the various situations, a general procedure can be performed by expressing the characteristic function as

$$\Phi(U,V)=\Phi(U,V)_{N_1}\Phi(-U,-V)_{N_2}, \quad \text{(B5)}$$

where $\Phi(U,V)_M$ is defined as

$$\Phi(U,V)_M=\langle e^{iU\mu\cos(2qa\delta_j)}e^{iV\mu\sin(2qa\delta_j)}\rangle^M. \quad \text{(B6)}$$

In Eqs. (B5) and (B6), the values of the integers N_1 and N_2 depend on the parity of both m and N. Indeed, for even m values, $N_1=N$ and $N_2=0$ and Eqs. (B5) and (B6) reduce to Eq. (B4). By contrast, for odd m values, $N_1=N_2=N/2$ when N is even and $N_1=(N-1)/2$, $N_2=(N+1)/2$ when N is odd. By performing the average over the variable $\delta_j=0,\pm1$ occurring into Eq. (B6) and weighted with the probability $p=1/3$, the function $\Phi(U,V)_M$ is written as

$$\Phi(U,V)_M=\sum_{r=0}^{M}\sum_{s=0}^{M-r}\frac{C_M^r C_{M-r}^s}{3^M}e^{iUX_r}e^{iVY_{r,s}}, \quad \text{(B7)}$$

where C_N^p is the usual binomial coefficient and

$$X_r=\mu[r+(M-r)\cos(2qa)],$$
$$Y_{r,s}=\mu(2s+r-M)\sin(2qa). \quad \text{(B8)}$$

At this step, by inserting Eq. (B7) into Eq. (B5) and by performing an inverse Fourier transform, it is straightforward to obtain the required probability distribution $h(X,Y)$ and then to deduce the distribution of the random quantum probability $S(N)$. The final result is given in Eq. (22).

[1] G. E. Moore, Electronics **38**, 114 (1964).
[2] R. Landauer, Z. Phys. B: Condens. Matter **68**, 217 (1987).
[3] Y. Imry and R. Landauer, Rev. Mod. Phys. **71**, S306 (1999).
[4] M. Buttiker, IBM J. Res. Dev. **32**, 63 (1988).
[5] N. Agrait, C. Untiedt, G. Rubio-Bollinger, and S. Vieira, Phys. Rev. Lett. **88**, 216803 (2002).
[6] S. Datta, *Electronic Transport in Mesoscopic Systems* (Cambridge University Press, Cambridge, 1995).
[7] J. I. Pascual, J. Mendez, J. Gomez-Herrero, A. M. Baro, N. Garcia, and Vu Thien Binh, Phys. Rev. Lett. **71**, 1852 (1993).
[8] N. Agrait, J. G. Rodrigo, and S. Vieira, Phys. Rev. B **47**, 12 345 (1993).
[9] J. G. Dash and J. Ruvalds, *Phase Transition in Surface Films* (Plenum, New York, 1980).
[10] M. G. Lagally, *Kinetics of Ordering and Growth at Surfaces* (Plenum, New York, 1980).
[11] L. W. Bruch, M. W. Cole, and E. Zaremba, *Physical Adsorption: Forces and Phenomena* (Clarendon, Oxford, 1997).
[12] C. B. Duke, *The First Thirty Years* (special issue), Surf. Sci. **299/300** (1994), and references therein.
[13] N. Sundaram, S. A. Chalmers, P. F. Hopkins, and A. C. Gossard, Science **254**, 1326 (1991).
[14] P. Gambardella, M. Blanc, H. Brune, K. Kuhnke, and K. Kern, Phys. Rev. B **61**, 2254 (2000).
[15] A. Dallmeyer, C. Carbone, W. Eberhardt, C. Pampuch, O. Rader, W. Gudat, P. Gambardella, and K. Kern, Phys. Rev. B **61**, R5133 (2000).
[16] G. Meyer and K. H. Rieder, Surf. Sci. **377–379**, 1087 (1997).
[17] G. Binnig and H. Rohrer, Rev. Mod. Phys. **71**, S324 (1999).
[18] G. Dujardin, R. E. Walkup, and Ph. Avouris, Science **255**, 1232 (1992).
[19] J. Gaudioso, H. J. Lee, and W. Ho, J. Am. Chem. Soc. **121**, 8479 (1999).
[20] H. J. Lee and W. Ho, Phys. Rev. B **61**, R16 347 (2000).
[21] L. J. Lauhon and W. Ho, Surf. Sci. **451**, 219 (2000).
[22] F. Picaud, C. Ramseyer, C. Girardet, and P. Jensen, Phys. Rev. B **61**, 16 154 (2000).
[23] F. Picaud, C. Ramseyer, C. Girardet, H. Brune, O. Roder, and K. Kern (unpublished).
[24] V. Pouthier and C. Girardet, Surf. Sci. **511**, 203 (2002).
[25] J. O. Vasseur, P. A. Deymier, L. Dobrzynski, and Jinhan Choi, J. Phys.: Condens. Matter **10**, 8973 (1998).
[26] P. W. Anderson, Phys. Rev. **109**, 1492 (1958).
[27] B. Kramer and A. MacKinnon, Rep. Prog. Phys. **56**, 1469 (1993).
[28] A. Bovier, J. Phys. A **25**, 1021 (1992).
[29] J. C. Flores, J. Phys.: Condens. Matter **1**, 8471 (1989).
[30] D. Dunlap, H. L. Wu, and P. Phillips, Phys. Rev. Lett. **65**, 88 (1990).

[31] P. Phillips and H. L. Wu, Science **252**, 1805 (1991).
[32] F. M. Izrailev and A. A. Krokhin, Phys. Rev. Lett. **82**, 4062 (1999).
[33] L. Tessieri and F. M. Izrailev, Phys. Rev. E **64**, 066120 (2001); Physica E **9**, 405 (2001).
[34] P. W. Anderson, D. J. Thouless, E. Abrahams, and D. S. Fisher, Phys. Rev. B **22**, 3519 (1980).
[35] A. Douglas Stone, J. D. Joannopoulos, and D. J. Chadi, Phys. Rev. B **24**, 5583 (1981).
[36] N. Kumar, Phys. Rev. B **31**, 5513 (1985).
[37] B. Shapiro, Phys. Rev. B **34**, 4394 (1986).
[38] A. Cohen, Y. Roth, and B. Shapiro, Phys. Rev. B **38**, 12 125 (1988).
[39] K. M. Slevin and J. B. Pendry, Phys. Rev. B **41**, 10 240 (1990).
[40] C. W. J. Beenakker, Rev. Mod. Phys. **69**, 731 (1997).
[41] M. Janssen, Phys. Rep. **295**, 1 (1998).
[42] J. S. Denbigh and N. Rivier, J. Phys. C **12**, L107 (1979).